

Document downloaded from:

<http://hdl.handle.net/10251/66823>

This paper must be cited as:

Gomis Vicens, J.; Carlos, L.; Bianco Prevot, A.; Teixeira, ACSC.; Mora Carbonell, M.; Amat Payá, AM.; Vicente Candela, R.... (2015). Bio-based substances from urban waste as auxiliaries for solar photo-Fenton treatment under mild conditions: Optimization of operational variables. *Catalysis Today*. 240(Part A):39-45. doi:10.1016/j.cattod.2014.03.034.



The final publication is available at

<http://dx.doi.org/10.1016/j.cattod.2014.03.034>

Copyright Elsevier

Additional Information

1 **Bio-based substances from urban waste as auxiliaries for**
2 **solar photo-Fenton treatment under mild conditions:**
3 **optimization of operational variables**

4 J. Gomis¹, L. Carlos², A. Bianco Prevot³, A. C. S. C. Teixeira⁴, M. Mora⁵, A.M. Amat¹,
5 R. Vicente¹, A. Arques^{1*}.

6 (1) Grupo de Procesos de Oxidación Avanzada, Dpto de Ingeniería Textil y Papelera,
7 Universitat Politècnica de València. Plaza Ferrándiz y Carbonell s/n, Alcoy, Spain.
8 aarques@txp.upv.es.

9 (2) Instituto de Investigaciones Fisicoquímicas Teóricas y Aplicadas (INIFTA), CCT-
10 La Plata-CONICET, Universidad Nacional de La Plata, Diag 113 y 64, La Plata,
11 Argentina.

12 (3) Dipartimento di Chimica, Università di Torino, Via Giuria 7, Torino, Italy.

13 (4) Escola Politécnica da Universidade de São Paulo, Av. Prof. Luciano Gualberto, tr.3,
14 380, São Paulo, Brasil.

15 (5) Dpto de Matemática Aplicada, Universitat Politècnica de València. Plaza Ferrándiz
16 y Carbonell s/n, Alcoy, Spain.

17 *Corresponding author: [mail: aarques@txp.upv.es](mailto:aarques@txp.upv.es), phone: ++34 966528417

18

19 **Abstract**

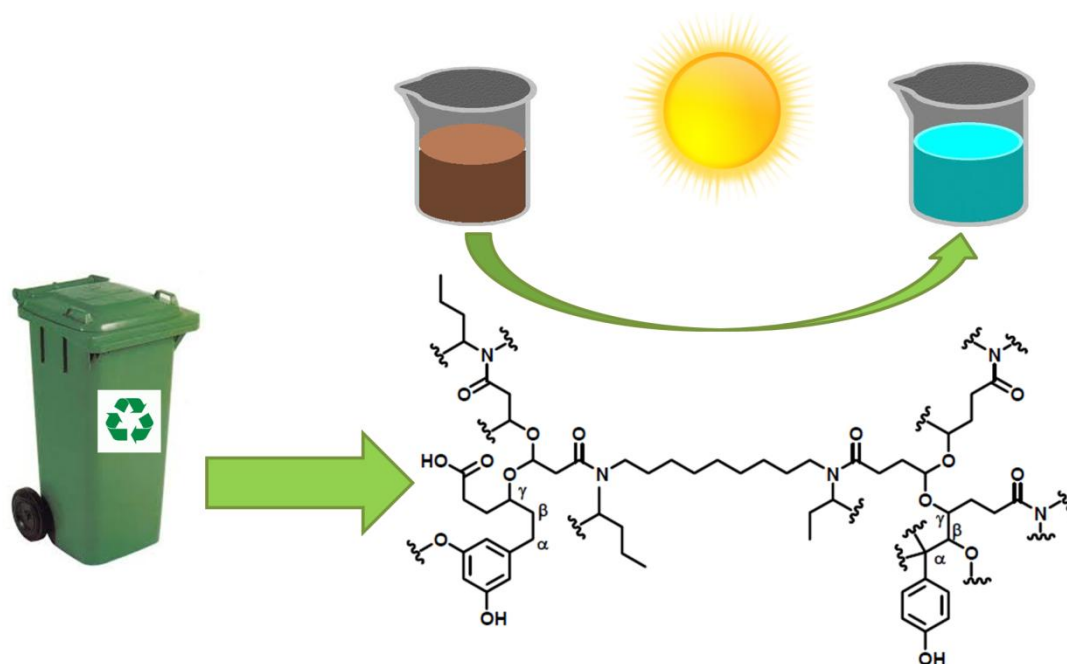
20 The use of soluble bio-based organic substances (SBO) obtained from urban wastes to
21 expand the pH region where the photo-Fenton process can be applied has been

22 investigated in this study. For this purpose, a mixture of six pollutants, namely
23 acetaminophen, carbamazepine, amoxicillin, acetemiprid, clofibric acid and caffeine, at
24 an initial concentration of 5 mg L^{-1} each, has been employed. Surface response
25 methodology, based on the Doehlert matrix, has shown to be a useful tool to determine
26 the effect of pH (in the range 3-7), concentration of SBO ($15\text{-}25 \text{ mg L}^{-1}$) and iron ($2\text{-}6$
27 mg L^{-1}) on the performance of the photodegradation of the studied pollutants, measured
28 by their half-life. Results indicate that, at high SBO concentration, the optimum pH
29 shifts in most cases to a higher value (between 3 and 4) and that a significant loss of
30 efficiency of the process was only observed at pH values above 5. An iron concentration
31 of $4\text{-}5 \text{ mg L}^{-1}$ and an amount of SBO of $19\text{-}22 \text{ mg L}^{-1}$ have been determined to be the
32 optimal conditions for the degradation of most of the studied pollutants at $\text{pH} = 5$.

33

34 Graphical abstract

35



36

37

38

39

40 **Highlights**

41 The effect of operational variables on the photo-Fenton process has been studied.

42 Surface response methodology has been applied for this purpose.

43 Soluble bio-organic substances enable an efficient photo-Fenton at higher pH

44

45 **Keywords**

46 Photo-Fenton, emerging pollutants, pH, soluble organic matter, SBO

47

48 **1. Introduction**

49 Wastes have deserved attention from researchers, as they could be a sustainable source

50 of materials with a wide range of potential applications [1]. In particular, soluble bio-

51 based organic substances (SBO) have been isolated from solid organic wastes submitted

52 to aging under aerobic fermentation conditions, following a process that involves

53 extraction of the soluble fraction at basic pH and posterior precipitation at acidic media

54 [2]. SBO are constituted by a mixture of macromolecules, which average molecular

55 weight ranges from 67 to 463 kg mol⁻¹; they consist of long aliphatic chains, aromatic

56 rings and several oxygen and nitrogen-containing functional groups [2]. Hence, these

57 materials show basic structural similarities with some macromolecules found in natural

58 organic matter (NOM), such as humic and fulvic acids, which play an important role in

59 photochemical processes leading to the self-remediation of ecosystems [3]. In this
60 context, determining the potential use of SBO for water detoxification is meaningful, as
61 this may be considered a green process since it valorises solid wastes as sources of
62 photoactive materials with similar properties as less available NOM. Information on this
63 issue is very scarce, and only some recent papers have been published reporting on the
64 ability of these compounds to act as photocatalysts in the degradation of chlorophenols
65 [4, 5], sulphonic acids [6], dyes [7, 8] or pharmaceuticals [9]. SBOs action can be
66 related to an enhanced photogeneration of reactive species; however, the strong screen
67 effect produced by these coloured materials negatively affects the degradation of
68 pollutants that can undergo direct photolysis. When simulated sunlight was employed as
69 irradiation source, the screen effect becomes predominating, thus making SBOs
70 unattractive as solar photocatalysts [9].

71

72 Alternatively, SBOs might also be employed as complexing agents to drive photo-
73 Fenton processes at mild conditions. Photo-Fenton is based on the ability of iron salts to
74 catalyse decomposition of hydrogen peroxide into highly oxidizing species (mainly
75 hydroxyl radicals, although other species might also contribute) in a process that is
76 accelerated by irradiation [10]. One major drawback of this process is the highly acidic
77 media required to avoid formation of non-active iron oxides or hydroxides. However,
78 some efforts have been recently made for the implementation of photo-Fenton at
79 circumneutral pH. This approach might be especially useful to treat emerging pollutants
80 (EPs) as a certain loss of efficiency in the generation of reactive species might be
81 acceptable in this case, as EPs are commonly found at low concentration, and hence
82 lesser amounts of oxidizing species are necessary [11, 12]. This strategy can be
83 improved by using chemical auxiliaries, able to form photoactive complexes, at mild

84 pH, with the iron added [13]. Humic acids are among the materials employed for this
85 purpose, because of their ability for iron complexation [13-16].

86

87 Because of their similarity with humic substances, SBOs are also candidates to extend
88 the application of photo-Fenton to pH conditions where iron ions are normally not
89 soluble. Indeed, photo-Fenton process in the presence of SBOs have been recently
90 shown to be able to remove a mixture of EPs at pH=5.2 [9]. Hence, a logical step
91 beyond is to determine the role of the operational parameters on the efficiency of the
92 process. For this purpose, a response surface methodology based on Doehlert design has
93 been chosen in this work in order to determine the effect of SBOs and iron
94 concentrations at the pH interval between 3, close to the optimal value, and 7. The
95 Doehlert design has been commonly employed as a chemometric tool, enabling to
96 minimize the number of experiments required to obtain the surface [17, 18]. The
97 mixture of EPs employed in previous work [9, 16] has been chosen as target solution:
98 acetaminophen, carbamazepine, amoxicillin, acetamiprid, clofibric acid and caffeine
99 (see Figure 1 for structures).

100

101 **2. Experimental**

102 2.1 Reagents

103 Acetaminophen, caffeine, amoxicillin, clofibric acid, carbamazepine and acetamiprid
104 were purchased from Sigma-Aldrich and used as received. Hydrogen peroxide (30%
105 v/v), ferric chloride, sulphuric acid and sodium hydroxide, were obtained from Panreac.
106 Water was Milli-Q grade.

107

108 The SBO employed in this work, namely CVT230, was obtained from urban biowastes
109 supplied by ACEA Pinerolese waste treatment plant (Pinerolo, Italy) following a
110 procedure detailed elsewhere [2, 19]. Briefly, the starting material was compost from
111 gardening-park trimming residues matured for 230 days: it was digested 4 h at 60 °C at
112 alkaline conditions (pH = 13) and 4 V/w water/solid ratio to favour hydrolysis of
113 organics. Alkaline hydrolyzed solution have been recognized as very similar to the
114 humic matter, in turn characterized by the presence of a dimensionally smaller fraction
115 (fulvic acid) soluble in all the pH range, and of a bigger one (humic acid), not soluble
116 below pH 3. Instead of separating the two fractions by means of pH variation, the size
117 difference was exploited. The recovered liquid phase was therefore circulated through a
118 polysulfone ultrafiltration membrane with 5 kD molecular weight cut-off to yield a
119 retentate with 5-10 % dry matter content. The membrane retentate was dried at 60 °C to
120 yield the final water soluble bio-based product (SBO). It contained 72.1% (w/w) of
121 volatile solids and the carbon content was 38.3 % (see [8] for further details).

122

123 2.2 Reactions

124 Experiments were performed in a 250 mL cylindrical Pyrex vessel irradiated with a
125 solar simulator (Sun 2000, ABET Technologies) equipped with a 550 W Xenon Short
126 Arc Lamp. A pyrex glass filter was used to cut off radiation below 300 nm (which only
127 accounted for a residual fraction of the lamp irradiance). The vessel was loaded with an
128 aqueous solution containing the six EPs at an initial concentration of 5 mg L⁻¹ each.
129 SBO concentration was varied in the range 15-25 mg L⁻¹; FeCl₃ was added to reach a
130 concentration of iron between 2 and 6 mg L⁻¹. The initial amount of hydrogen peroxide

131 was 2.2 mmol L⁻¹ in all cases, which is half the stoichiometric amount required to
132 mineralize the EPs; this concentration was employed in order to obtain a relatively slow
133 kinetics, which allows a better determination and comparison of illumination times
134 required to remove the EPs under the different conditions that have been studied. The
135 pH was adjusted to the desired value (3-7) by dropwise addition of either 0.1 mmol L⁻¹
136 NaOH or 0.1 mmol L⁻¹ H₂SO₄. Temperature was kept in the range 30-35 °C throughout
137 the reaction. Samples were periodically taken from the solution, filtered through a
138 polypropylene membrane (0.45µm) and diluted 1:1 with methanol.

139

140 Control experiments showed that direct photolysis of the pollutants was negligible
141 under the employed conditions and irradiation in the presence of H₂O₂ solely resulted in
142 a moderate degradation of amoxicillin (less than 20% after 200 min of irradiation).

143

144 2.3. Analysis

145 The concentration of each EP was determined by UPLC (Perkin Elmer model Flexar
146 UPLC FX-10). A Brownlee Analytical column (DB-C18) was employed as stationary
147 phase. The eluent consisted in a mixture of acetonitrile (A) and a 0.1% formic acid
148 aqueous solution (B); the relative amount of each solvent was changed following a
149 linear gradient, from 3% A to 70% A in 8 min; the flow rate was 0.3 mL min⁻¹.
150 Detection wavelengths were 205 nm (acetaminophen, amoxicillin, caffeine and
151 carbamazepine), 225 nm (clofibric acid) and 245 nm (acetamiprid). Identification and
152 quantification of the EPs were performed by comparison with standards.

153

154 2.4 Surface response methodology

155

156 In order to gain further insight into the effect of the studied operational variables (pH,
157 SBO and iron concentration), an experimental design methodology based on a Doehlert
158 array [20]. In this case, a total of 15 experiments (k^2+k+1 , where k is the number of
159 analysed variables, 3 in this study, plus two replicates of the central point) were
160 performed. Experimental conditions of all experiments are found in Table 1. The
161 software Statgraphics Centurion XVI was used for response surface model fitting by
162 means of the least squares method. The illumination time required to degrade each
163 pollutant to 50% of its initial concentration ($t_{50\%}$) was used as response, which was
164 obtained from the plot of the relative EP concentration vs. illumination time.

165

166 3. Results and discussion

167

168 Plots of the relative concentration of each EP vs illumination time were obtained for
169 each experiment (see Figure 2 for an example). Considering an illumination time of 90
170 minutes, the results show complete removal of all EPs for the experiments carried out at
171 pH 3. At pH 5, removals between 90 and 100% were obtained for all EPs except
172 acetamiprid, for which removals in the range 54-68.5% were obtained. These results
173 confirm the efficiency of the photo-Fenton reaction under acidic and mildly acidic
174 conditions, the later favoured by the presence of SBOs. Finally, maximum percent
175 removals between 5.7 and 64.7% were obtained for the experiments carried out at pH 7,
176 again the lowest removals after 90 minutes of illumination (5.7-21%) corresponding to
177 acetamiprid. These trends show that the choice of a response like the illumination time

178 necessary to obtain pollutant removals of 90% or greater could not be considered for all
179 EPs and pH for the conditions used in the present study (pollutants initial
180 concentrations, H₂O₂ and iron concentrations) and in some cases would require too long
181 illumination times to be observed.

182

183 As a result, the illumination time required for the removal of 50% of each pollutant
184 (t_{50%}) was considered for every experiment (Table 1). From the practical point of view,
185 the response t_{50%} is not submitted to phenomena such as lack of hydrogen peroxide or
186 changes in the experimental conditions that can affect the kinetic behaviour and/or
187 reproducibility (mainly under the less efficient conditions, where too long illumination
188 times would be required). Based on the response values in Table 1, six three-dimensional
189 full quadratic response surface models were obtained, one for each EP (see Table 2,
190 Equations I-A to I-F). For all EPs the values of the determination coefficient (R²) were
191 high (92.4; 97.4; 98.1; 97.1; 95.9; and 99.4% for amoxicillin, carbamazepine,
192 acetamiprid, clofibric acid, caffeine, and acetaminophen, respectively), indicating good
193 agreement between experimental and calculated values of the response variable. In each
194 case, the values of the residuals (differences between calculated and measured values of
195 t_{50%}) as a function of measured values were randomly distributed with error zero with
196 zero mean.

197

198 The corresponding ANOVA tables (see Supplementary Data, Tables T1-T6) and the
199 Pareto charts (Figure 3) show that except for acetaminophen, the only significant effect
200 on t_{50%} at 95% confidence level (*p*-values < 0.05) was due to pH, as expected, being the
201 reaction faster at lower pH values; the quadratic effect of this variable was significant,

202 indicating the important curvature of the response surfaces. For acetaminophen, the
203 quadratic effect of SBO concentration was also significant. Therefore, simplified model
204 equations for $t_{50\%}$ were fitted by considering the effect of pH only, as presented in Table
205 2 (cf. Equation II-A to II-F) (see Supplementary Data, Tables T7-T12 for the
206 corresponding ANOVA tables). In comparison with the complete model equations, in
207 most cases the values of R^2 decreased as the simplified fitted models exhibit lack-of-fit
208 and fail to predict $t_{50\%}$ for the experiments in which the effects of SBO and Fe(III)
209 concentrations on the response are important (see Supplementary Data, Figures F1-F6).
210 In other words, the effect of pH on the response is so pronounced that it masks the
211 effects of the other variables, especially that of SBO concentrations for some pH
212 conditions. For that reason, in order to discuss some trends concerning the effects of
213 SBO and Fe(III) concentrations and to better determine the pH domain where the photo-
214 Fenton could be applied, the complete fitted response surface models were considered,
215 and two-dimensional contour plots were built for each EP by fixing [SBO] at the higher
216 and lower values.

217

218 Figure 4A shows data obtained for carbamazepine. At low SBO concentration, a fast
219 decrease in the efficiency of photo-Fenton with increasing pH is observed, as the line
220 corresponding to $t_{50\%} = 20$ min can be found at a pH of ca. 4 and that of 60 min at a pH
221 of approximately 5.5. At low pH (below 4) an increase in [Fe(III)] results in a slight
222 enhancement of the process. This behaviour could be attributed to differences in iron
223 availability: at acidic medium, higher amounts of iron can be kept in solution, what
224 results in a faster degradation reaction; however, above pH = 4, SBOs are not able to
225 prevent efficiently iron precipitation and reaction rate decreases.

226

227 In contrast, at the highest SBO concentration (25 mg L^{-1}) a different trend can be found:
228 the loss of efficiency of the process occurs at higher pH, as differences are not acute in
229 the pH range 3-5.5, what suggests that SBOs are useful materials to apply the photo-
230 Fenton reaction at milder pH conditions. Furthermore, the optimum pH shifted to higher
231 values (ca. 4). This might indicate a change in the photo-Fenton mechanism, in which
232 the key species is not only $\text{Fe}(\text{OH})^{2+}$ (responsible for the optimal pH value of 2.8), but
233 photoactive iron-SBO complexes might also contribute. Modification of the optimum
234 pH has already been described when species able to modify iron complexation are
235 present. For instance, at high concentration of chloride, photo-Fenton exhibits the best
236 performance at a pH slightly above 3 [21]. In addition, changes in photo-Fenton
237 mechanism at circumneutral values and or in the presence of chelating agent, such as
238 EDTA [22, 23] or citrate [24, 25], have been proposed, eventually changing the key
239 species [26]. Interestingly, when ethylenediamine- $\text{N,N}'$ -disuccinic acid (EDDS) was
240 used as complexing agent, best results were reached at neutral or even slightly basic
241 medium; this variation was attributed to a completely different mechanism in which
242 superoxide plays a key role [27]. In the case of SBOs, experiments carried out with
243 chemical probes have shown that other species, in addition to $\bullet\text{OH}$ radicals, are
244 responsible for pollutants degradation [8-9].

245

246 Results obtained with clofibrac acid (Figure 4E) and caffeine (Figure 4F) are very
247 similar to carbamazepine and for these compounds the photo-Fenton reaction showed to
248 be efficient until pH slightly above 5 at $[\text{SBO}]$ of 25 mg L^{-1} . In fact, previous
249 experiments involving mild photo-Fenton conditions with non-complexed iron or in the
250 presence of humic substances or SBOs have demonstrated that they follow similar
251 behaviour with only quantitative differences. Acetamiprid (Figure 4D) is the most

252 recalcitrant compound towards the photo-Fenton process [8, 9]. This low reactivity
253 results in a poor efficiency of photo-Fenton, which quickly decreases with increasing
254 pH (the line of $t_{50\%} = 60$ is at pH ca. 5 at low and high SBO concentrations).
255 Amoxicillin, on the other hand, is the most reactive among the EPs towards photo-
256 Fenton and at $[SBO] = 25 \text{ mg L}^{-1}$ shows the highest efficiency at pH = 5 and reaction
257 rate did not decrease significantly until values close to 7 (Figure 4C). Finally, for
258 acetaminophen (Figure 4B) a slow but continuous decrease in reaction rate with
259 increasing pH is observed (line $t_{50\%} = 60$ min at pH = 6). In fact, in a previous study [9]
260 this compound has been shown to have a different reactivity in comparison to the other
261 EPs, in which other species than $\bullet\text{OH}$ play an important role.

262

263 Based on those results, it could be hypothesised that the presence of SBOs modifies the
264 photo-Fenton mechanism and, although some differences in the individual behaviour of
265 each EP have been evidenced, the process can be extended, in most cases, at least up to
266 pH = 5. Hence it is interesting to determine at this pH value the role of $[\text{Fe(III)}]$ and
267 $[SBO]$ in view of optimizing these variables. Contour plots obtained at pH = 5 for all six
268 EPs can be observed in Figure 5; the corresponding fitted equations are shown in Table
269 2 (cf. Table 2, Equations III-A to III-F) (see Supplementary Data for the ANOVA
270 tables, Tables T13-T18). In general, an optimum can be found in the region 4-5 mg L^{-1}
271 of iron and 19-22 mg L^{-1} of SBO, which should be considered as the best conditions for
272 the removal of the EPs from water by the photo-Fenton process. Under those conditions,
273 $t_{50\%}$ was ca. 20 min for all EPs, except for amoxicillin ($t_{50\%} < 10$ min) and for
274 acetamiprid, which was the most refractory; in fact, acetamiprid was the only compound
275 which did not show a minimum for $t_{50\%}$ in the studied region.

276

277 The behaviour of SBO can be explained by considering that this species is necessary to
278 keep iron in solution and to allow the photo-Fenton process at pH = 5. However, beyond
279 a given point the role of SBO might be detrimental because it can act as scavenger of
280 the reactive species, competing with the pollutants, or because of a light screening effect
281 related to its brown colour. In the case of iron, it seems that amounts above 4 mg L⁻¹
282 play a negative role; this can be attributed to the faster precipitation of iron to form
283 oxides/hydroxides, which, in turn, decrease the photo-Fenton efficiency.

284

285 **Conclusions**

286

287 SBOs have been demonstrated as useful materials to allow the implementation of the
288 photo-Fenton processes at higher pH values (at least 5). This can be due to the ability of
289 these materials to complex iron, thus avoiding its precipitation as oxides or hydroxides.
290 The surface response methodology enabled to study the effect of iron, SBO and pH on
291 the process. Surface responses obtained at pH = 5 showed that optimal conditions of
292 Fe(III) and SBO concentrations were in the range 4-5 mg L⁻¹ and 19-22 mg L⁻¹
293 respectively. Extending this methodology to other variables (e.g. H₂O₂ concentration) or
294 other compounds is a logical step forward.

295

296 Although a mechanistic study for such a complex system falls beyond the aim of this
297 study, our results seem to point to a modification of the photo-Fenton mechanism in
298 which the optimum pH shifts to higher values (in most cases in the range 3-4, slightly
299 above the optimal value described for photo-Fenton, 2.8). Furthermore, some
300 differences in the behaviour of each EP have been identified, which may be explained

301 by their reactivity with the new species formed, whose nature remains to be elucidated.
302 Hence, further research on the mechanistic issues of the process seems meaningful.

303

304 Finally, future work is also required to study the process at pH = 5 under real sunlight at
305 pilot plant with more realistic aqueous matrixes, estimating values such as H₂O₂
306 consumption, irradiation time or changes in biocompatibility, in order to better assess
307 the real applicability of this methodology.

308

309 **Acknowledgements**

310 The authors want to thank the financial support of the European Union (PIRSES-GA-
311 2010-269128, EnvironBOS) and Spanish Ministerio de Educación y Ciencia
312 (CTQ2012-38754-C03-02). Juan Gomis would like to thank UPV for his FPI grant
313 (2010-07).

314

315 **References**

- 316 [1] R.A.D. Arancon, C.S.K. Lin, K.M. Chan, T.H.Kwan, R. Luque, Energy Sci.
317 Technol, 1 (2013) 53-71.
- 318 [2] E. Montoneri, D. Mainero, V. Boffa, D.G. Perrone, C Montoneri, Int J. Global
319 Environ. Issues 11 (2011) 170-196.
- 320 [3] S. K. Khetan, T.J. Collins, Chem. Rev. 107 (2007) 2319-2364.
- 321 [4] A. Bianco Prevot, P. Avetta, D. Fabbri, E. Laurenti, T. Marchis, D.G. Perrone, E.
322 Montoneri, V. Boffa, ChemSusChem 4 (2011) 85-90.

- 323 [5] P. Avetta, F. Bella, A. Bianco Prevot, E. Laurenti, E. Montoneri, A. Arques, L.
324 Carlos, *Sustainable Chem. Eng.* 1 (2013) 1545-1550.
- 325 [6] P. Avetta, A. Bianco Prevot, D. Fabbri, E. Montoneri, L. Tomasso, L. Chem. Eng. J.
326 197 (2012) 193-198.
- 327 [7] A. Bianco Prevot, D. Fabbri, E. Pramauro, C. Baiocchi, C. Medana, E. Montoneri,
328 V. Boffa, *J. Photochem. Photobiol. A: Chem.* 209 (2010) 224-231.
- 329 [8] J. Gomis, R.F. Vercher, A.M. Amat, D.O. Martire, M.C. González, A. Bianco-
330 Prevot, E. Montoneri, A. Arques, L. Carlos. *Catal. Today*, 209 (2013) 176-180.
- 331 [9] J. Gomis, A. Bianco Prevot, E. Montoneri, M.C. González, A.M. Amat, D.O.
332 Mártire, A. Arques, L. Carlos, *Chem. Eng. J.* 235 (2014) 236-243.
- 333 [10] J.J. Pignatello, E. Oliveros, A. MacKay, *Critical Rev. Environ. Sci. Technol.* 36
334 (2006) 1-84.
- 335 [11] I. Carra, J.L. Casas López, L. Santos-Juanes, S. Malato, J.A. Sánchez Pérez, *Chem*
336 *Eng. J.* 224 (2013) 67-74.
- 337 [12] N. De la Cruz, L. Esquius, D. Grandjean, A. Magnet, A. Tungler, L.F. de
338 Alencastro, C. Pulgarin. *Water Res.* 47 (2013) 5836-5845.
- 339 [13] N. Klamerth, S. Malato, A. Agüera, A. Fernández-Alba. *Water Res.* 47 (2013) 833-
340 840.
- 341 [14] N. Klamerth, S. Malato, M.I. Maldonado, A. Agüera, A. Fernández-Alba, *Catal.*
342 *Today* 161 (2011) 241-246.

- 343 [15] A. Bernabeu, R.F.Vercher, L.Santos-Juanes, P.J.Simón, C.Lardín, M.A.Martínez,
344 J.A. Vicente, R.González, C.Llosá, A.Arques, A.M. Amat, Catal. Today, 161 (2011)
345 235-240.
- 346 [16] A. Bernabeu, S. Palacios, R.Vicente, R. Vercher, S.Malato, A. Arques, A.M. Amat.
347 Chem Eng. J. 198-199 (2012) 65-72.
- 348 [17] D.H. Doehlert. Uniform shell designs. J R Stat Soc.,Ser C 19 (1970) 231–239.
- 349 [18] M.A. Bezerra, R.E. Santelli, E.P. Oliveira, L.S.Villar, L.A. Escaleira, Talanta 76
350 (2008) 965–977.
- 351 [19] Montoneri E., Boffa V., Savarino P., Perrone D.G., Ghezzi M., Montoneri C.,
352 Mendichi R., Waste Manage. 31 (2011) 10-17
- 353 [20] S. L. C. Ferreira, W. N. L. dos Santos, C. M. Quintella, B. B. Neto, J. M. Bosque-
354 Sendra, Talanta 63 (2004) 1061-1067.
- 355 [21] A. Machulek, J.E.F. Moraes, C. Vautier-Giongo, C.A. Silverio, L.C. Friedrich,
356 C.A.O. Nascimento, M.C. González, F Quina, Environ. Sci. Technol. 41 (2007) 8459–
357 8463.
- 358 [22] N. Klamerth, S. Malato, A. Agüera, A. Fernández-Alba, G. Mailhot, Environ. Sci.
359 Technol. 46 (2012) 2885-2892.
- 360 [23] J.D. Rush, W.H. Koppenol, J. Biol. Chem. 261 (1986), 6730-6733.
- 361 [24] M.R.A. Silva, A.G. Trovó, R.F.P. Nogueira, J. Photochem. Photobiol A: Chem.
362 191 (2007) 187-192
- 363 [25] H. Katsumata, S. Kaneco, T. Suziki, K. Ohta, Y. Yobiko, J. Photochem. Photobiol
364 A: Chem.180 (2006) 38-45.

- 365 [26] S.J. Hug, O. Leupin, *Environ. Sci. Technol.* 37 (2003), 2734-2742.
- 366 [27] W. Huang, M. Brigante, F. Wu, C. Mousty, K. Hanna, G. Mailhot, *Environ. Sci.*
- 367 *Technol.* 47 (2013) 1952-1959
- 368

Exp number	[Fe(III)]	[SBO]	pH	A	B	C	D	E	F
1	4	20	5	21.6	25.8	14.4	57.6	24.3	25.5
1'	4	20	5	18.1	24.9	16	54.1	24.6	26.6
1''	4	20	5	15	22	10	48.8	20.4	23.2
2	6	20	5	23.8	26.6	12.8	59.5	28.2	31.3
3	5	25	5	27.8	33.8	22	68.9	32.1	36.4
4	2	20	5	27.9	28.4	24.4	57	29.5	35.1
5	3	15	5	34.4	41.6	26.3	83.9	40.3	47.1
6	5	15	5	33.3	36.4	24.4	68.9	36.1	39.6
7	3	25	5	27.5	33	22.3	65.8	33.7	35.8
8	5	21.7	7	129.4	86.3	111.5	320	133.3	207.5
9	3	21.7	7	88.4	82.1	62.4	218	87.4	109.7
10	4	16.7	7	154	75.5	174.3	242.7	156.4	150
11	3	18.3	3	2.3	3.3	2.3	6.4	2.7	3.1
12	5	18.3	3	1.7	1.5	1	3.9	2.1	1.8
13	4	23.3	3	1.3	2.4	1.3	4.6	1.8	2.1

369

370 Table 1: Experimental points used to obtain the response surface (Doehlert matrix). The
371 concentrations of SBO and iron are expressed as mg L⁻¹; data given in the last six
372 columns correspond to the time (in min) required to decrease concentration of each EP
373 to 50% of the initial value for carbamazepine (A), acetaminophen (B), amoxicillin (C),
374 acetamiprid (D), clofibric acid (E) and caffeine (F)

375

Compound	Equation
Carbamazepine	$t_{50\%} \text{ (min)} = 248.38 - 40.37 \cdot [\text{Fe}] - 8.52 \cdot [\text{SBO}] - 51.39 \cdot \text{pH} + 1.90 \cdot [\text{Fe}]^2 + 0.07 [\text{Fe}] [\text{SBO}] + 5.14 \cdot [\text{Fe}] \cdot \text{pH} + 0.43 [\text{SBO}]^2 - 2.08 \cdot [\text{SBO}] \cdot \text{pH} + 10.28 \cdot \text{pH}^2 \quad (R^2 = 0.974) \text{ (I-A)}$ $t_{50\%} \text{ (min)} = 106.29 - 62.86 \text{ pH} + 9.34 \text{ pH}^2 \quad (R^2 = 0.915) \text{ (II-A)}$ $t_{50\%} \text{ (min)} = 239.50 - 17.38 \cdot [\text{Fe}] - 17.88 [\text{SBO}] + 1.90 [\text{Fe}]^2 + 0.43 [\text{SBO}]^2 + 0.07 [\text{Fe}] [\text{SBO}] \quad (R^2 = 0.930) \text{ (III-A)}$
Acetaminophen	$t_{50\%} \text{ (min)} = 318.33 - 15.36 \cdot [\text{Fe}] - 22.79 \cdot [\text{SBO}] - 32.82 \cdot \text{pH} + 0.82 \cdot [\text{Fe}]^2 + 0.30 [\text{Fe}] [\text{SBO}] + 0.50 [\text{Fe}] \text{ pH} + 0.45 [\text{SBO}]^2 + 0.71 \cdot [\text{SBO}] \cdot \text{pH} + 3.64 \cdot \text{pH}^2 \quad (R^2 = 0.994) \text{ (I-B)}$ $t_{50\%} \text{ (min)} = 3.98 - 9.21 \text{ pH} + 2.89 \text{ pH}^2 \quad (R^2 = 0.963) \text{ (II-B)}$ $t_{50\%} \text{ (min)} = 253.57 - 13.20 \cdot [\text{Fe}] - 19.60 [\text{SBO}] + 0.82 [\text{Fe}]^2 + 0.45 [\text{SBO}]^2 + 0.3 [\text{Fe}] [\text{SBO}] \quad (R^2 = 0.972) \text{ (III-B)}$
Amoxicillin	$t_{50\%} \text{ (min)} = 56.92 - 41.63 \cdot [\text{Fe}] + 3.80 \cdot [\text{SBO}] - 19.34 \cdot \text{pH} + 1.28 \cdot [\text{Fe}]^2 + 0.08 [\text{Fe}] [\text{SBO}] + 6.23 \cdot [\text{Fe}] \cdot \text{pH} + 0.36 [\text{SBO}]^2 - 4.19 \cdot [\text{SBO}] \cdot \text{pH} + 10.69 \cdot \text{pH}^2 \quad (R^2 = 0.924) \text{ (I-C)}$ $t_{50\%} \text{ (min)} = 123.65 - 70.42 \text{ pH} + 9.91 \text{ pH}^2 \quad (R^2 = 0.794) \text{ (II-C)}$ $t_{50\%} \text{ (min)} = 199.27 - 13.98 \cdot [\text{Fe}] - 15.04 [\text{SBO}] + 1.28 [\text{Fe}]^2 + 0.36 [\text{SBO}]^2 + 0.08 [\text{Fe}] [\text{SBO}] \quad (R^2 = 0.879) \text{ (III-C)}$
Acetamidiprid	$t_{50\%} \text{ (min)} = 966.42 - 83.28 \cdot [\text{Fe}] - 40.02 \cdot [\text{SBO}] - 206.76 \cdot \text{pH} + 1.19 \cdot [\text{Fe}]^2 + 0.91 \cdot [\text{Fe}] \cdot [\text{SBO}] + 12.29 \cdot [\text{Fe}] \cdot \text{pH} + 0.69 \cdot [\text{SBO}]^2 + 1.77 \cdot [\text{SBO}] \cdot \text{pH} + 18.59 \cdot \text{pH}^2 \quad (R^2 = 0.981) \text{ (I-D)}$ $t_{50\%} \text{ (min)} = 180.38 - 110.88 \text{ pH} + 17.47 \text{ pH}^2 \quad (R^2 = 0.946) \text{ (II-D)}$ $t_{50\%} \text{ (min)} = 440.30 - 28.18 \cdot [\text{Fe}] - 32.03 [\text{SBO}] + 1.19 [\text{Fe}]^2 + 0.69 [\text{SBO}]^2 + 0.91 [\text{Fe}] [\text{SBO}] \quad (R^2 = 0.915) \text{ (III-D)}$
Clofibric acid	$t_{50\%} \text{ (min)} = 242.78 - 40.30 \cdot [\text{Fe}] - 9.39 \cdot [\text{SBO}] - 44.58 \cdot \text{pH} + 1.44 \cdot [\text{Fe}]^2 + 0.13 [\text{Fe}] [\text{SBO}] + 5.70 \cdot [\text{Fe}] \cdot \text{pH} + 0.44 [\text{SBO}]^2 - 2.06 \cdot [\text{SBO}] \cdot \text{pH} + 9.40 \cdot \text{pH}^2 \quad (R^2 = 0.971) \text{ (I-E)}$ $t_{50\%} \text{ (min)} = 88.28 - 54.22 \text{ pH} + 8.51 \text{ pH}^2 \quad (R^2 = 0.907) \text{ (II-E)}$ $t_{50\%} \text{ (min)} = 246.10 - 14.80 \cdot [\text{Fe}] - 18.67 [\text{SBO}] + 1.44 [\text{Fe}]^2 + 0.44 [\text{SBO}]^2 + 0.13 [\text{Fe}] [\text{SBO}] \quad (R^2 = 0.955) \text{ (III-E)}$
Caffeine	$t_{50\%} \text{ (min)} = 702.53 - 79.39 \cdot [\text{Fe}] - 25.36 \cdot [\text{SBO}] - 147.13 \cdot \text{pH} + 2.02 \cdot [\text{Fe}]^2 + 0.41 [\text{Fe}] [\text{SBO}] + 12.04 \cdot [\text{Fe}] \cdot \text{pH} + 0.50 \cdot [\text{SBO}]^2 + 0.65 [\text{SBO}] \text{ pH} + 12.44 \cdot \text{pH}^2 \quad (R^2 = 0.959) \text{ (I-F)}$ $t_{50\%} \text{ (min)} = 126.86 - 75.73 \text{ pH} + 11.41 \text{ pH}^2 \quad (R^2 = 0.890) \text{ (II-F)}$ $t_{50\%} \text{ (min)} = 310.83 - 25.51 \cdot [\text{Fe}] - 22.51 [\text{SBO}] + 2.03 [\text{Fe}]^2 + 0.50 [\text{SBO}]^2 + 0.41 [\text{Fe}] [\text{SBO}] \quad (R^2 = 0.984) \text{ (III-F)}$

376

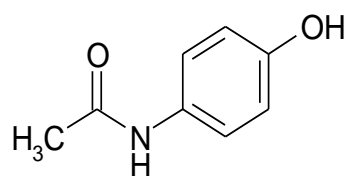
377 Table 2: Response surface models obtained for each EP, where the values of the

378 variables are specified in their original units. (I) refer to the complete fitted model, (II)

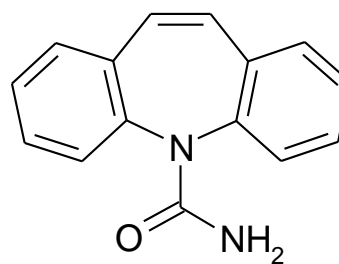
379 to the simplified fitted model without the non-significant variables, and (III) to the fitted

380 model considering only the experiments performed at pH 5

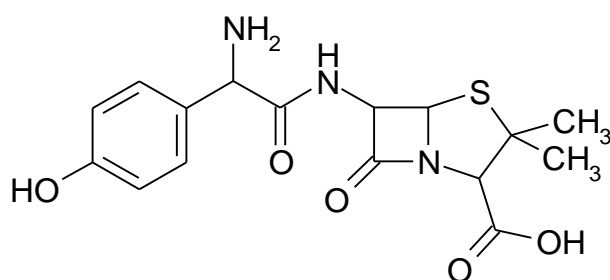
381 Figure 1: Chemical structures of EPs used in this study



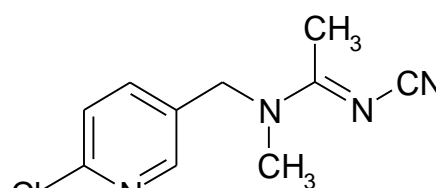
Acetaminophen



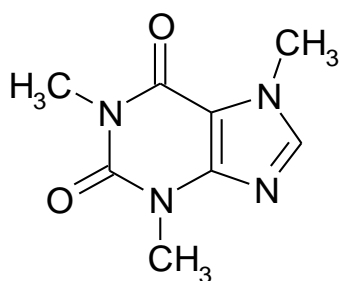
Carbamazepine



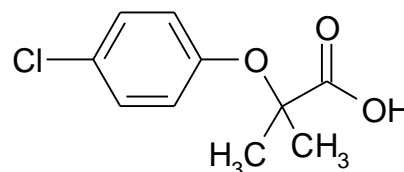
Amoxicillin



Acetamiprid



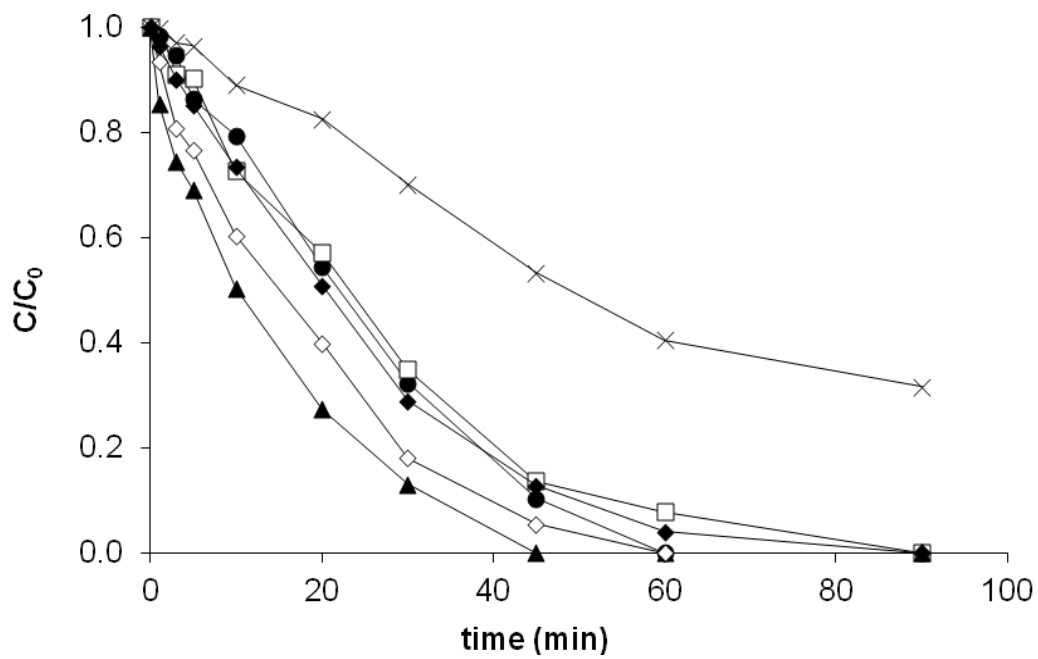
Caffeine



Clofibric acid

382 Figure 2: Example of the photodegradation of a mixture of 6 EPs by means of the
383 photo-Fenton reaction. Plot of the relative concentration vs time: amoxicillin (▲),
384 acetaminophen (●), acetamiprid (×), caffeine (□), clofibric acid (◆) and carbamazepine
385 (◇). Data correspond to the central point ($[SBO] = 20 \text{ mg L}^{-1}$, $[Fe(III)] = 4 \text{ mg L}^{-1}$, pH =
386 5)

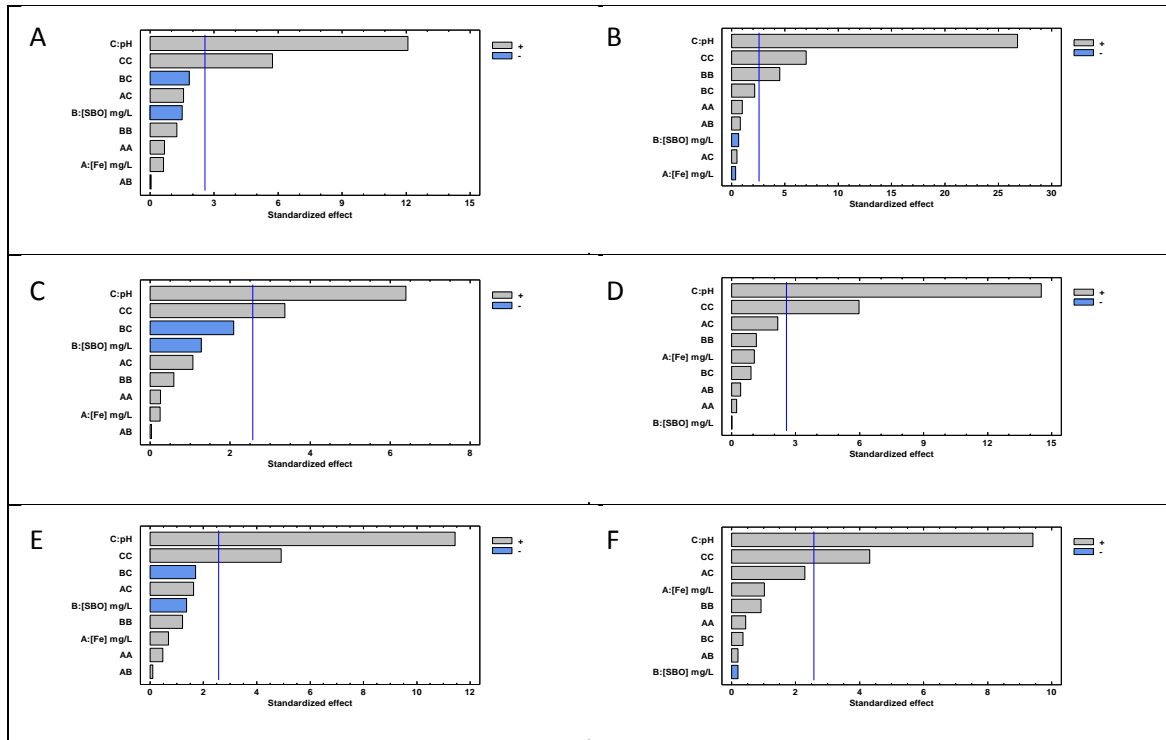
387



388

389

390 Figure 3: Pareto charts for the response $t_{50\%}$ (min) obtained for the photo-Fenton
 391 degradation of EPs in the presence of SBO. The EPs are carbamazepine (A),
 392 acetaminophen (B), amoxicillin (C), acetamiprid (D), clofibric acid (E) and caffeine (F)



393

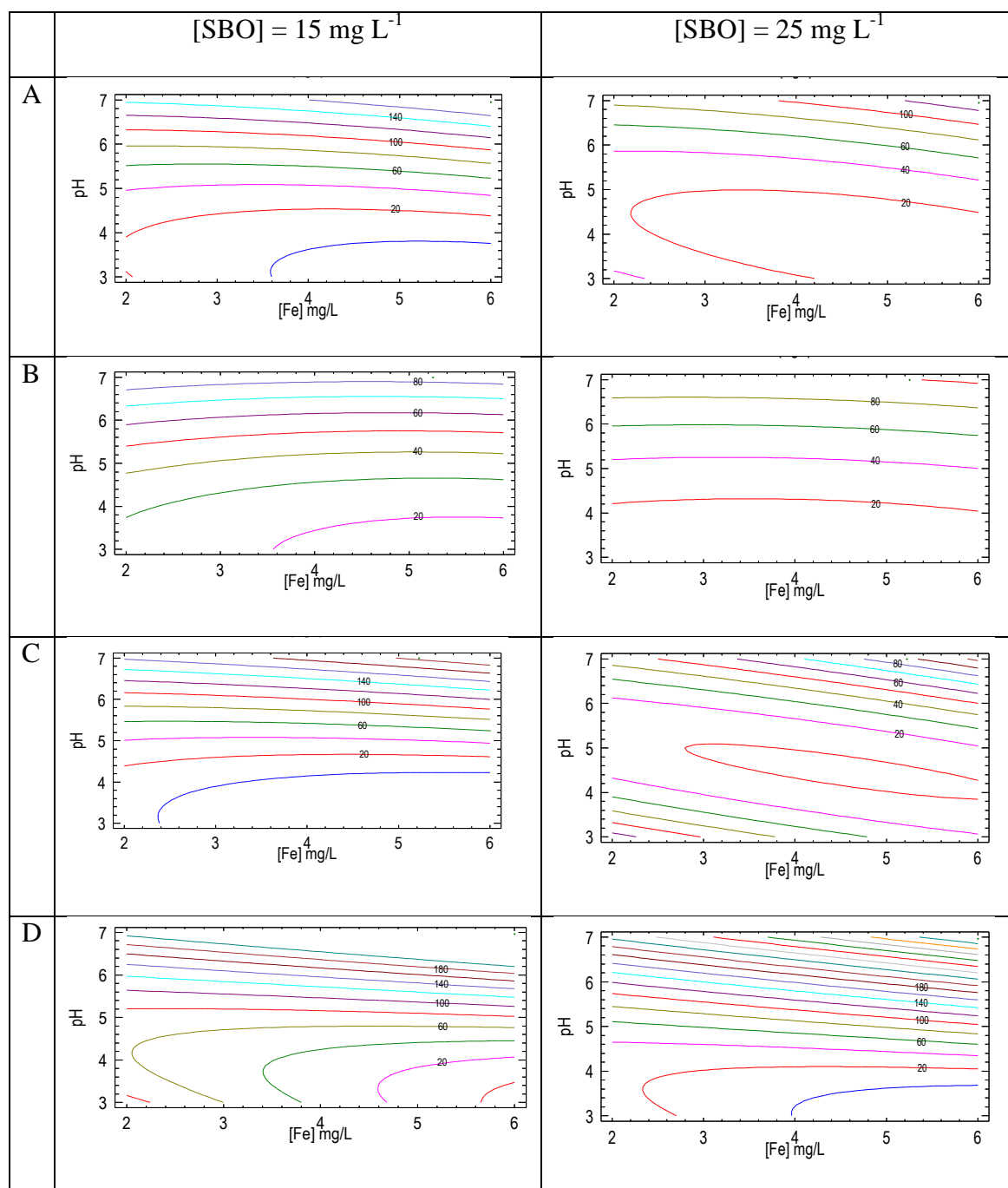
394

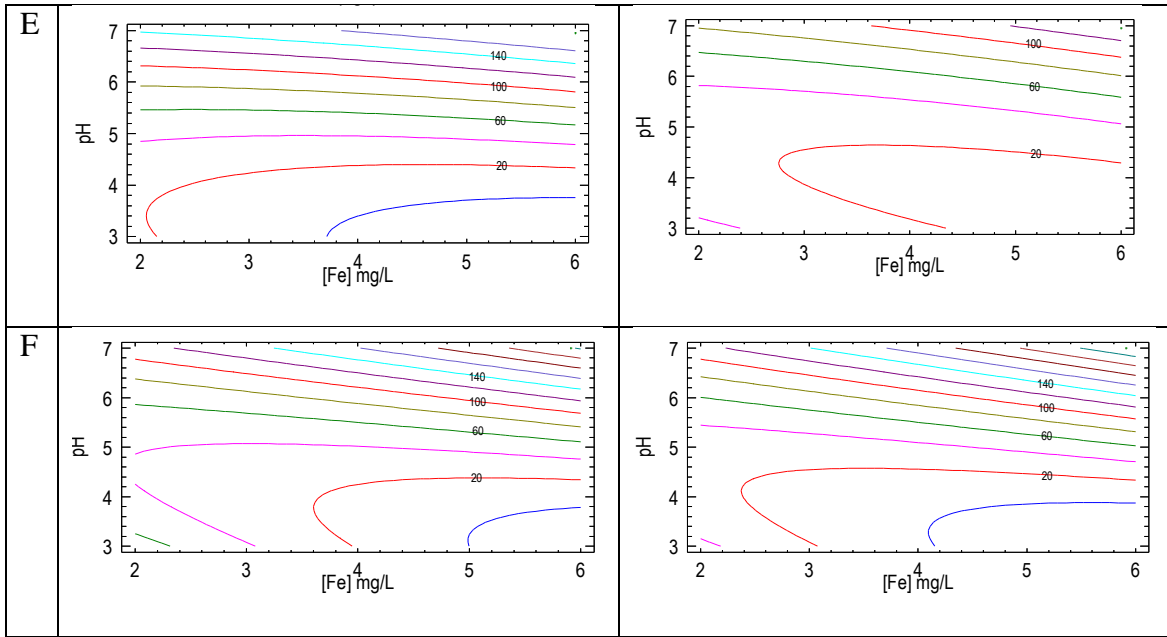
395 Figure 4: Contour plots for $t_{50\%}$ (min) obtained for the photo-Fenton degradation of EPs

396 in the presence of SBO. The EPs are carbamazepine (A), acetaminophen (B),

397 amoxicillin (C), acetamiprid (D), clofibric acid (E) and caffeine (F)

398





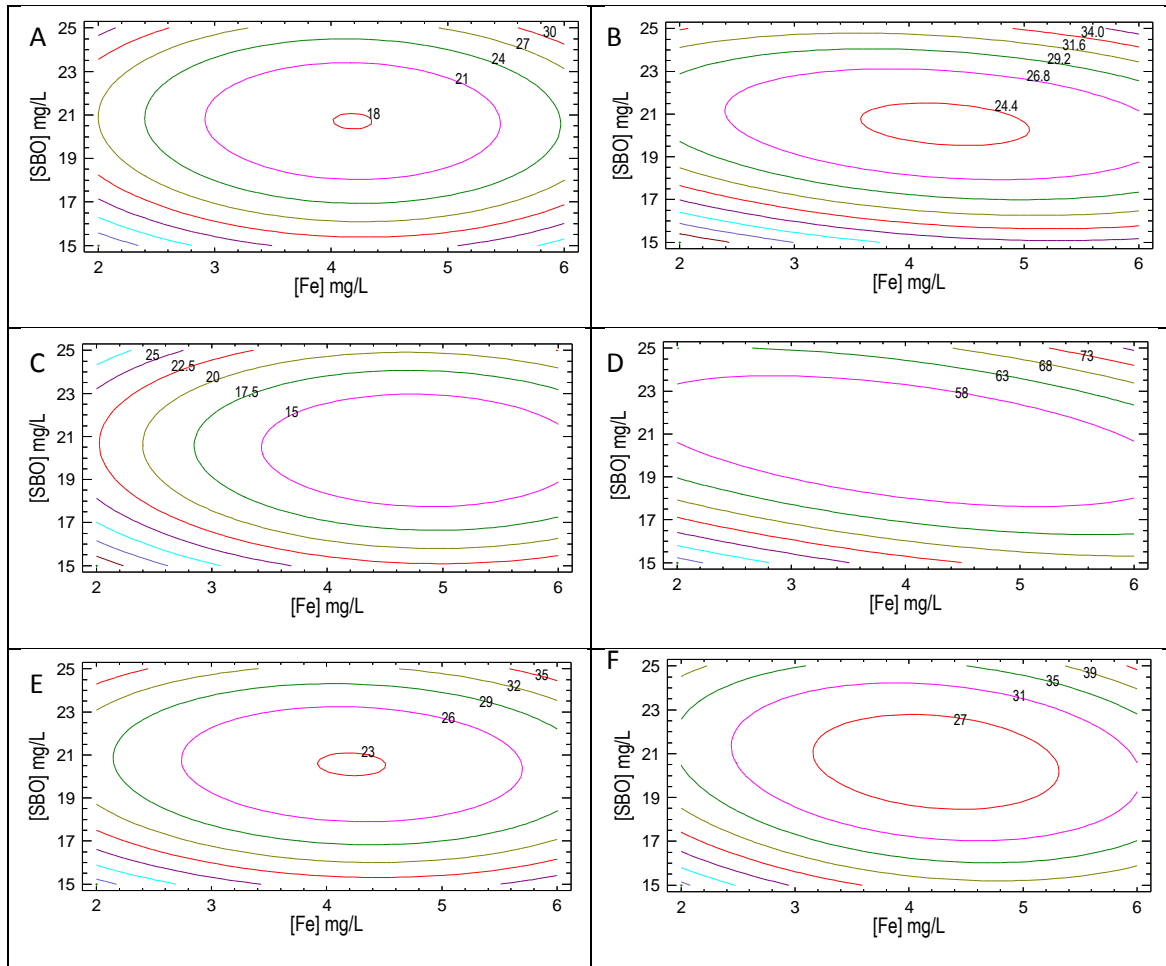
399

400

401

402

403 Figure 5: Contour plots for $t_{50\%}$ (min) obtained for the photo-Fenton degradation of EPs
404 at pH = 5. The EPs are carbamazepine (A), acetaminophen (B), amoxicillin (C),
405 acetamiprid (D), clofibric acid (E) and caffeine (F)



406

e-component

[Click here to download e-component: supplementary data.docx](#)